nutraceuticals

MDPI

Article

Analysis of Osmotic Pump-Administered Xylitol in a Syngeneic Mouse Melanoma Model

Mark Cannon [1,2,*], Elizabeth Dempsey [3], Ashlee Cosantino [2] and Nayereh Ghoreishi [3]

[1] Department of Otolaryngology, Feinberg School of Medicine, Northwestern University, Chicago, IL 60611, USA
[2] Pediatric Dentistry, Ann and Robert Lurie Children's Hospital, Chicago, IL 60611, USA; acosantino@luriechildrens.org
[3] Developmental Therapeutics Core, Northwestern University, Chicago, IL 60611, USA; elizabeth.dempsey@northwestern.edu (E.D.); nayereh.ghoreishi@northwestern.edu (N.G.)
* Correspondence: markcannon@northwestern.edu

Abstract

The present study used a syngeneic mouse model of malignant melanoma to evaluate the inhibitory efficacy of continuous xylitol administration via a subcutaneous osmotic minipump. The B16F10 syngeneic model for malignant melanoma consisted of 6–8-week-old C57BL/6 male mice subcutaneously injected with 5×10^5 B16F10 cells suspended in 100 µL PBS in the right flank. The mice were randomly assigned to two groups: Group 1 was the treatment group, which received 10% *w*/*v* xylitol in saline-loaded pumps ($n = 10$), while Group 2 was the control group, which received saline-loaded pumps ($n = 10$). ALZET 2004 minipumps were implanted subcutaneously in the left flank of B16F10-injected mice once more than 50% of all mice developed palpable tumors. After pump implantation surgery, the mice were monitored daily and weighed 2–3× times per week. Tumor sizes were measured with calipers 2–3× per week, and all mice were euthanized when their tumors became too large (20 mm on any axis or 2000 mm^3). The tumor size growth was reduced by approximately 35% by volume in the xylitol-treated group which was not statistically significant. The xylitol group had a longer survival time, but this was not statistically significant (Kaplan–Meier), as was the case with the survival analysis by the Cox proportional hazards model. The metabolomic analysis suggests that xylitol significantly alters the tumor's metabolism, potentially affecting the host immune response.

Keywords: ALZET osmotic minipumps; malignant melanoma; xylitol; syngeneic mouse model

check for updates

Academic Editor: Masayoshi Yamaguchi

Received: 4 July 2025
Revised: 4 October 2025
Accepted: 13 October 2025
Published: 3 November 2025

Citation: Cannon, M.; Dempsey, E.; Cosantino, A.; Ghoreishi, N. Analysis of Osmotic Pump-Administered Xylitol in a Syngeneic Mouse Melanoma Model. *Nutraceuticals* **2025**, *5*, 36. https://doi.org/10.3390/nutraceuticals5040036

Copyright: © 2025 by the authors. Licensee MDPI, Basel, Switzerland. This article is an open access article distributed under the terms and conditions of the Creative Commons Attribution (CC BY) license (https://creativecommons.org/licenses/by/4.0/).

1. Introduction

Xylitol is a prebiotic polyol that has been used for preventive dental care for many decades. It is considered natural and is generally regarded as a safe food additive or supplement [1]. It has long been used as a substitute for ordinary table sugar due to its sweetness and taste profile, which are similar to those of sucrose [2]. In 1975, Mäkinen et al. first reported that xylitol significantly reduced dental caries by inhibiting the growth of *Streptococcus mutans* [3]. Since then, clinical studies have shown that xylitol products reduce the oral microbiome levels of *S. mutans*, decrease plaque accumulation, and decrease the incidence of dental caries in children [4–6]. Total or partial substitution of sucrose with xylitol in the human diet reportedly results in more than an 85% reduction in the incidence of dental caries [7]. According to Mäkinen et al., most *S. mutans* strains transport

xylitol into the cell via the phosphotransferase system, which is then phosphorylated to xylitol-5-phosphate and expelled from the cell [8,9]. This energy-consuming pathway is thought to inhibit *S. mutans* and other energy-dependent pathogens [10]. Numerous studies have demonstrated the efficacy of xylitol in preventing caries and inhibiting the growth of periodontal pathogens [11,12]. Additionally, xylitol provides microbial balance by maintaining a healthy gut microbiome, starting with the oral gateway microbiome, which supports innate immunity and disease resistance [13–16].

The microbiome's influence on cancer development and treatment has recently been recognized [17]. As a result, research on complex microbial communities and the mechanisms through which microbiota influence cancer prevention, carcinogenesis, and anticancer therapy has significantly increased. Therefore, researchers are considering the urgent development of next-generation prebiotics and probiotics designed to target specific diseases [18]. Healthcare professionals can utilize prebiotics, probiotics, and postbiotics to prevent and treat diseases such as cancer [19]. The hallmarks of cancer are immune elimination and escape, both of which can be partly bacteria-dependent, shaping immunity by mediating host immunomodulation [20]. Additionally, host immunity regulates the microbiome by modulating bacterial associated signaling to influence tumor surveillance [21]. Cancer immunotherapy, including immune checkpoint blockade, appears to have heterogeneous therapeutic effects in different individuals, partially attributed to the microbiota [22]. Personalized medicine will require a better understanding of the microbiota and their interaction with cancer cells. The manipulation of gut microbiota with prebiotics to improve cancer therapeutic responses may prove indispensable for future cancer treatment [23].

When administered orally and systemically, xylitol inhibits the growth of cancer cells [24–26]. Because xylitol is utilized by healthy human cells and exhibits almost no side effects, it may be a safe supplement for inhibiting the proliferation of cancer cells [27,28]. Xylitol also decreased tumor vascularization by inhibiting angiogenesis. Increased vascularization supports tumor growth and possibly cancer metastasis [29]. Xylitol is also a natural substance, and humans are reported to produce approximately 15 g of xylitol per day in the liver [30]. Xylitol is converted by mitochondrial xylitol dehydrogenase into a precursor of the tricarboxylic acid cycle. Xylitol dehydrogenase on the cristae metabolizes xylitol to xylulose, which converts NADP to NADPH [31]. Many plants naturally contain measurable amounts of xylitol, including blueberries, strawberries, plums, cauliflower, and oatmeal [32,33]. This is in addition to the production of xylitol by the human liver from glucose via the pentose phosphate pathway [32]. Interestingly, there is some overlap between the list of xylitol-containing foods and the American Heart Association's list of "heart-healthy" foods [33]. Also, xylitol has been suggested to help prevent diabetes and act as an anti-inflammatory agent [34,35].

Previously published research on animal models has reported positive results in inhibiting cancer cell lines and cancer xenografts with xylitol supplementation [36]. Combination treatments with olive oil phenolic compounds and xylitol have also been reported to be potentially beneficial [37]. The first phase of cancer research, which involves identifying potential therapeutic agents, typically utilizes animal models [38,39]. Therefore, the present study used a syngeneic mouse model for human malignant melanoma to evaluate the inhibitory efficacy of xylitol (a commercial product from Xlear, American Fork, UT, USA) delivered via ALZET osmotic mini pumps.

2. Materials and Methods

The B16F10 Syngeneic Model consisted of 6–8-week-old C57BL/6 male mice (Charles River Laboratories, Raleigh, NC, USA subcutaneously injected with 5×10^5 B16F10 cells (ATCC CRL-6475) suspended in 100 µL PBS into the right flank. Mice were monitored

for tumor development and randomized according to tumor volume and body weight for implantation surgery. The mice were then randomly assigned to two groups: Group 1 was the xylitol group, receiving 10% w/v xylitol in saline-loaded minipumps (n = 10), while Group 2 was the control group, receiving saline-loaded minipumps (n = 10). ALZET mini pumps (Model 2004, Campbell, CA, USA) were implanted in B16F10-injected mice once more than 50% of the mice developed palpable tumors approximately 50 mm. ALZET osmotic pumps were loaded with a 10% w/v xylitol solution in saline or saline vehicle controls. The pumps were primed at 37 °C for 48 h before the implantation surgery. All mini pump surgeries had to be completed in one day, and the mini pumps were loaded more than 40 h before surgery. The minipumps should have released xylitol for 28 days until pump depletion. Xylitol was delivered as a 10% (w/v) solution in saline using ALZET model 2004 osmotic minipumps (flow rate 0.26 μL/h 28-day duration). This corresponds to 0.624 mg/day, or approximately 25 mg/kg/day for a 25 g mouse and the total pump volume (μL uL) was 200. All animal procedures were conducted in accordance with the ethical standards and approved protocols of Northwestern University. Mice were housed under a 12:12-h light/dark cycle with access to standard chow (Envigo 7912. Indianapolis, IN, USA) and water ad libitum. Envigo Teklad 7912 mouse chow does not contain added sucrose as a distinct ingredient. The carbohydrate content is approximately 44.3% available carbohydrate, primarily derived from complex sources such as ground corn, oats, wheat middlings, and soybean meal, without refined sugars like sucrose.

Twenty mice underwent surgery to implant ALZET minipumps and were group-housed before and after surgery. Each mouse was placed under isoflurane anesthesia (~3%) and then given preoperative analgesia (SQ: 20 mg/kg meloxicam, line block of 2 mg/kg 0.1% bupivacaine). Under sterile conditions, an incision of approximately 1 cm was made in the lower left flank. Pumps were placed subcutaneously in the lower left flank, and for most mice, the surgical incision was located caudal to the mini pump. The incisions were closed using 2 to 3 wound clips. The mice were monitored 2× daily for the first 48 h post-operation. After minipump implantation surgery, the mice were monitored and weighed 2–3× weekly. Tumor sizes were measured with calipers 2–3× per week, and all mice were euthanized when their tumors reached a diameter of 20 mm on any axis or a volume of 2000 mm^3. The mice were randomized as assignments by allocation concealment. The technician measuring the mice's tumor was blinded to each determination, and the samples sent to histology and metabolomics were also blinded. Euthanasia was determined by tumor size and mouse distress, and the decision was blinded. Exclusion criteria were limited to prespecified humane endpoints (tumor size $\geq$ 20 mm or signs of distress). No animals were replaced. Animals were housed in groups, with allocation at the individual animal level, not at the cage level. Cage was not modeled as a random effect given the short study duration and the fact that 50% of control animals reached endpoint by day 10 and 50% of xylitol animals by day 15.

All tumor volumes were measured by caliper and calculated by the following modified ellipsoidal formula:

$$\text{Tumor volume} = 1/2\ (\text{length} \times \text{width2})$$

or V = (L × W2)/2; L is the length, and W is the width. L is the greatest longitudinal diameter (length), and W is the greatest transverse diameter (width). This formula is the standard used by the Developmental Therapeutics Core at Northwestern University, Evanston, IL, USA.

The excised tumors were measured and then carefully cut in half, with one half sent for histological analysis and the other for metabolomic analysis. In addition to tumor tissue, draining lymph nodes were collected and sent for comparative, qualitative histological analysis. The osmotic minipumps were collected and weighed for data analysis. After

euthanasia, tumor tissue was collected for two studies: metabolomics (tissue flash-frozen in liquid nitrogen) and histopathology, where the tissue was fixed in formalin for H&E staining to assess general morphology and IHC staining.

Rodent CO_2 euthanasia was performed according to IACUC protocol. Animals were not combined from different cages to reduce stress, and when euthanizing an entire cage, the animals remained in their original housing. The maximum number of mice per cage was five, and the CO_2 flow rate per mouse cage was 3 L/min until one minute after breathing stopped. Euthanasia was confirmed by cervical dislocation. Immediately following euthanasia, tumors were harvested, sectioned, and one-half fixed in 10% neutral-buffered formalin for 48 h. Tumors were embedded in paraffin, sectioned into 4–5 µm-thick sections, placed on microscopic slides, and stained with hematoxylin and eosin (H&E) by the Mouse Histology and Phenotyping Laboratory of Northwestern University. Microscopic slides were imaged using an Olympus BX45 microscope with an Olympus DP28 digital camera (Olympus, Center Valley, PA, USA). Digital images were visualized using Olympus cellSens imaging software (version 4.2).

Metabolomic samples were analyzed using high-performance liquid chromatography, high-resolution mass spectrometry, and Tandem mass spectrometry (HPLC-MS/MS). Specifically, the system consisted of a Thermo Q-Exactive, in line with an electrospray source, and an Ultimate3000 (Thermo) series HPLC, comprising a binary pump, degasser, and autosampler outfitted with an Xbridge Amide column (Waters; dimensions: 3.0 mm × 100 mm, particle size: 3.5 µm). The mobile phase A contained 95% (*v*/*v*) water, 5% (*v*/*v*) acetonitrile, 10 mM ammonium hydroxide, 10 mM ammonium acetate, pH = 9.0; B was 100% Acetonitrile. The gradient was as follows: 0 min, 15% A; 2.5 min, 30% A; 7 min, 43% A; 16 min, 62% A; 16.1–18 min, 75% A; 18–25 min, 15% A with a flow rate of 150 µL/min. The capillary of the ESI source was set to 275 °C, with sheath gas at 35 arbitrary units, auxiliary gas at five arbitrary units, and the spray voltage at 4.0 kV. In positive/negative polarity switching mode, an m/z scan range from 60 to 900 was chosen, and MS1 data was collected at a resolution of 70,000. The automatic gain control (AGC) target was set at 1 × 106, and the maximum injection time was 200 ms. The top 5 precursor ions were subsequently fragmented in a data-dependent manner, using the higher-energy collisional dissociation (HCD) cell set to 30% normalized collision energy in MS2 at a resolution of 17,500. Besides matching m/z, metabolites are identified by matching either retention time with analytical standards and/or MS2 fragmentation pattern. Xcalibur 4.1 software and Tracefinder 4.1 software from Thermo Fisher Scientific (Thermo Fisher Scientific, Waltham, MA, USA) were used for data acquisition and analysis. MetaboAnalyst software 6.0 can be used for statistical and functional data analysis and Mendelian randomization for causal inference.

3. Results

The survival of the xylitol group appeared 40% longer than that of the control group, but not by a statistically significant amount (Chi-square 1.859, df 1, $p = 0.1727$)—see Figure 1. The difference in the survival rate was not statistically significant, perhaps due to the sample size. The Kaplan–Meier survival curve analysis demonstrated an insignificant difference between the groups. Survival analysis by Cox proportional hazards model gave a hazard ratio of 0.65 (95% CI: wide, $p = 0.17$), indicating a lower risk of death in the xylitol group, though this difference was also not statistically significant.

The tumor volumes were significantly different on days 8 and 15 ($p < 0.05$) but not on day 10. The growth of the tumor was reduced by approximately 35% by volume (See Figure 2) in the xylitol group, with a statistically significant difference, but only on certain days of the tumor growth. The weight gain in the xylitol groups was also significantly

less than in the control group (see Figure 3) due to the decreased tumor volume. The average tumor volume for the control group was 2651.34 mm^3, and 1796.12 mm^3 for the xylitol group, making the xylitol tumors 68% of the control tumor volume. The mice had been randomized into the control and xylitol groups according to the volume of the tumor present to ensure equal distribution before insertion of the minipumps.

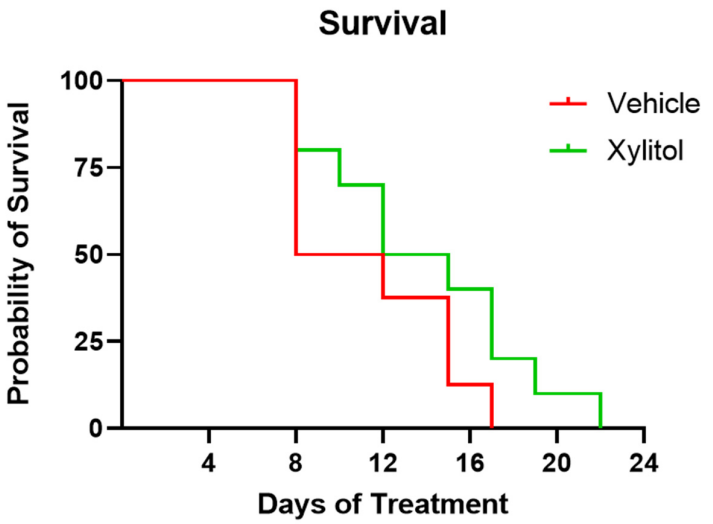


Figure 1. Kaplan–Meier Survival Plot of Xylitol versus Control. Survival days plotted for xylitol versus vehicle control. Although the xylitol mice survived 35% longer, a comparison of Survival Curves with the Log-rank (Mantel–Cox) test (Chi square 1.859 df 1 $p = 0.17270$) demonstrated a non-significant result. Days 10–12 of the study uniquely present survivability, weight gain, and tumor volume data that are inconsistent.

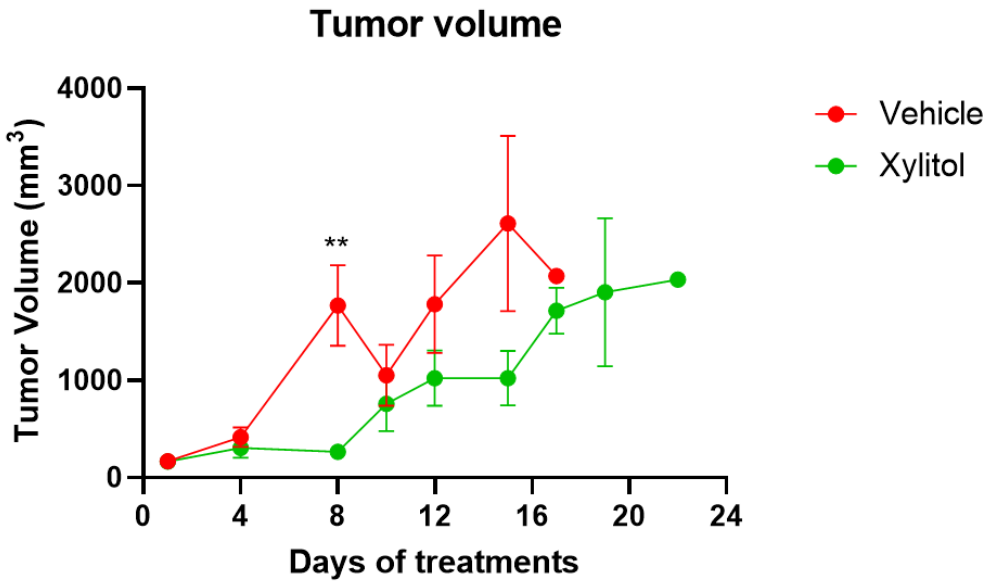


Figure 2. Tumor Volumes on Days of Treatment. The tumor volumes in the control (vehicle) and xylitol groups values are presented as +/− the Standard Error of the Means. *t*-test statistical analysis was used to compare tumor volumes between groups on the same day. No statistical difference is noted on Day 10. However, on Day 8, the difference in volumes was significant, with a *p*-value < 0.01 (**).

Upon initiation of the intervention with osmotic pumps, the average weight of the mice was 25.9 g, the xylitol group being slightly less in weight but not significantly so. All mice had the same diet and water supplied. Although the xylitol from the osmotic pumps provided extra calories, the amount was negligible. The level of xylitol the mice

received was not toxic and was well-tolerated. Published animal and human studies on long-term food intake have not reported any changes, except that xylitol, when substituted for sucrose, aids in weight management. Sucrose was not part of the mouse diet, and no clinical toxicity was attributable to xylitol. We interpreted group weight differences cautiously and related them to tumor burden.

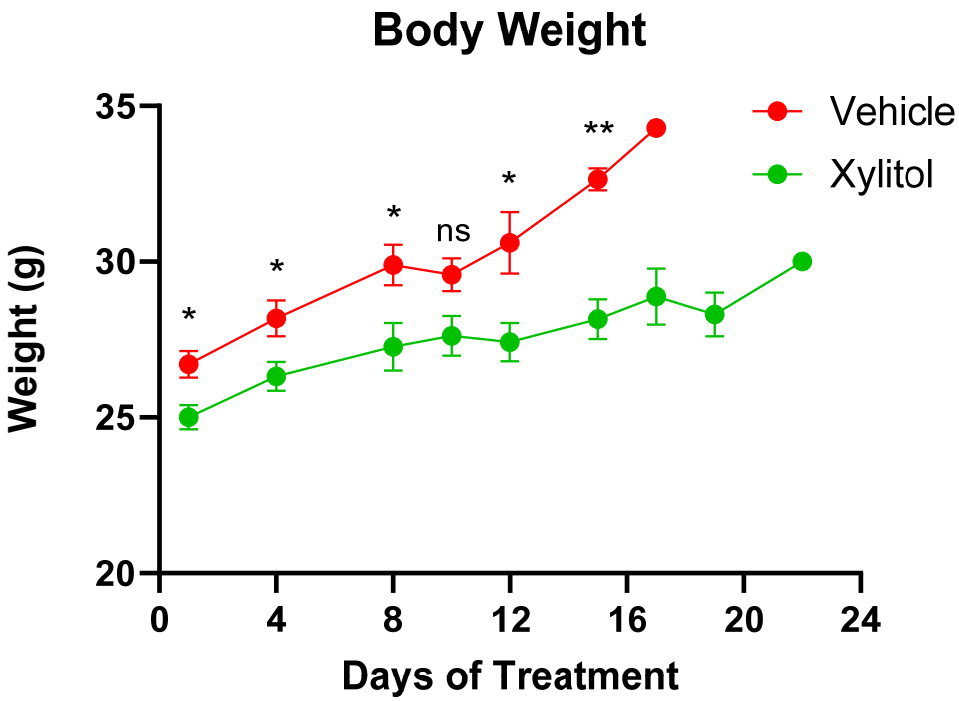


Figure 3. Animal Weights. Animal weights in the Control (Vehicle) and Xylitol groups are presented as mean ± SEM. A *t*-test was performed to compare the average weight between the groups on the same day. A *p*-value < 0.05 is denoted with (*), *p*-value < 0.01 is denoted with (**), and "ns" indicates no significant differences. There is no significant difference on Day 10.

The metabolomic analysis heatmap (Figure 4) demonstrated that xylitol reduced the tumor production of histidine, acetylcholine, GTP, ATP/dGTP, and UDP, possibly impacting the host's immune response to tumor cells by reactive oxygen species production [40]. Significant differences existed between the xylitol and control groups. Note that proline, NMN, and XMP increase with the vehicle group. Additionally, the xylitol group exhibited decreases in dopamine, epinephrine, and putrescine levels compared to the control group. The results of the statistical analysis (*t*-test) comparing the control to the xylitol groups are shown in Table 1. Xylitol significantly increases dATP, ATP/dGTP, CDP, SAICAR, acetoacetic acid, N1-acetylspermine, F-1, 6/2, 6-DP, and spermidine metabolites in the tumor compared to the saline control.

The histological samples (see Figure 5a,b) demonstrated areas of extensive intratumoral necrosis (arrows) with viable tumor cells surrounding blood vessels (asterisks). Scattered mitotic figures were present throughout the viable fraction of tumors (arrowheads). There were no discernible histopathological differences between the vehicle and the xylitol groups; however, metabolomic changes that result in increased cancer cell sensitivity to innate immunity may not be apparent in histological sections. However, the tumor size in the vehicle group was measurably larger (Figure 3). Tumors in both treatment groups exhibited considerable variability in intratumoral necrosis (viable tumor fraction) and mitotic indices. The nature of the necrosis in the tumors was characteristic of aggressive tumor cells that outgrow their blood supply, resulting in necrosis of the cells farthest from

the blood vessels. Lymph node tissue demonstrated metastasis in one lymph node in each group, with no significant differences.

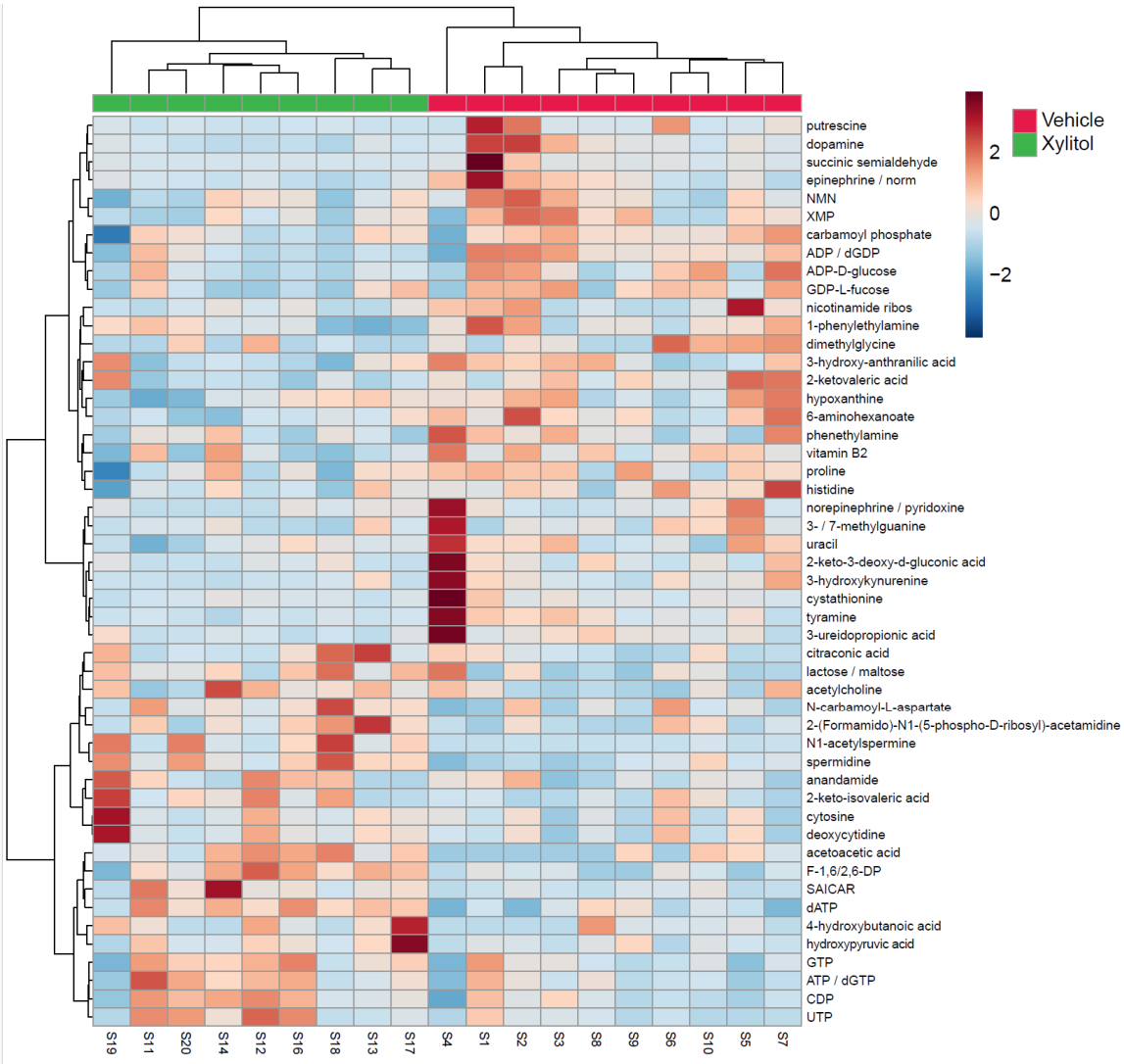


Figure 4. Metabolomics Results. Metabolomics analysis of tumors comparing xylitol to vehicle-treated syngeneic mice models. The heatmap displays the fifty most common metabolites, with the xylitol group denoted as green and the control group as red. The metabolites are listed on the right side of the heatmap. Each animal number is listed in the bottom row. Significant differences exist between the xylitol and control groups. Note the increases in proline, NMN, and XMP in the vehicle group. The xylitol group had increases in UTP, CDP, ATP, and GTP.

Table 1. Metabolite Log Values in Tumors: Xylitol vs. Saline Control.

Metabolite	***t*.stat**	***p*.Value**
dATP	−4.1503	0.00067
spermidine	−3.7167	0.001715
F-1,6/2,6-DP	−3.2851	0.004368
N1-acetylspermine	−3.1546	0.005786
6-aminohexanoate	2.983	0.008352
acetoacetic acid	−2.8922	0.010128

Table 1. *Cont.*

Metabolite	*t*.stat	*p*.Value
dopamine	2.5854	0.019254
UTP	−2.4726	0.024271
ADP/dGDP	2.4571	0.025048
SAICAR	−2.3512	0.031036
tyramine	2.3357	0.032018
CDP	−2.3348	0.032075
epinephrine/normetanephrine	2.2182	0.040446
vitamin B2	2.1843	0.043235
2-ketovaleric acid	2.1751	0.044027
ATP/dGTP	−2.1645	0.044953

Metabolites in **BOLD** are increased in the control tumors by the log value in the second column compared to the xylitol group. The *t* test *p* values are listed in the third column. Significant differences exist between the vehicle and xylitol tumor metabolites.

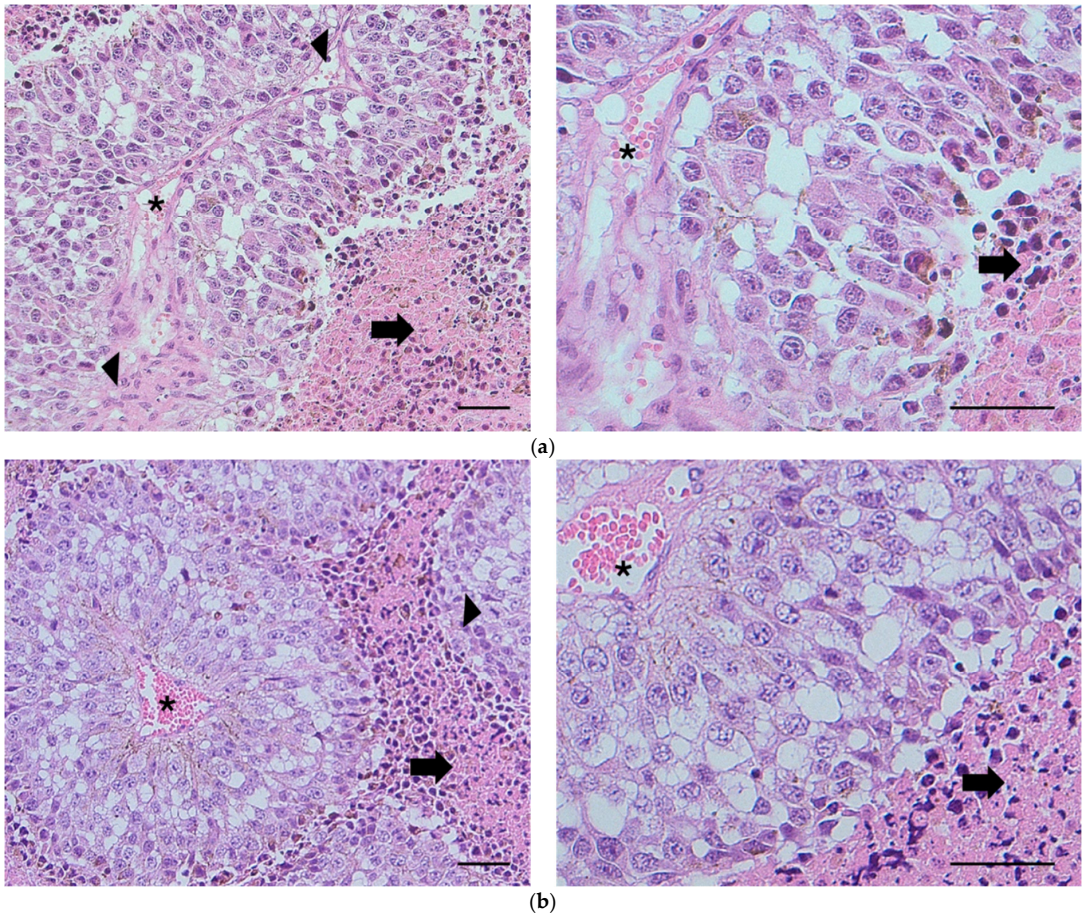


Figure 5. (**a**) Histology. Subcutaneous tumor from Mouse 736 (vehicle). Extensive intratumoral necrosis (arrows) with viable tumor cells surrounding blood vessels (asterisks). Scattered mitotic figures are found throughout the viable fraction of the tumor (arrowheads). H&E, bar = 100 µm. (**b**) Subcutaneous tumor from Mouse 729 (xylitol). Microscopic features are comparable to those observed in mice administered the vehicle. Extensive intratumoral necrosis (arrows) with viable tumor cells surrounding blood vessels (asterisks). Scattered mitotic figures are found throughout the viable fraction of the tumor (arrowhead). H&E, bar = 100 µm. The histological report did not denote any significant differences between the two groups.

4. Discussion

The present study was part of a series of syngeneic models aimed at evaluating the effects of xylitol on tumor cell proliferation and determining any improvement in the survival of the subject mice. Although the raw data looked promising, the results were not statistically significant. However, metabolomics revealed a significant change in metabolites within the tumor when xylitol was administered instead of a saline control. This finding is consistent with our previous research and other published scientific articles [19,26,27]. The metabolomic analysis revealed that xylitol induced a metabolic response in the tumor, potentially enhancing the host immune response to reactive oxygen species generated by innate immune cells.

N1-acetylspermine is a polyamine derivative that plays a crucial role in cellular metabolism and function. Formed through the acetylation of spermine, it is involved in various physiological processes, including regulating gene expression, stabilizing nucleic acids, and modulating enzyme activities [41]. This metabolite is associated with cell growth, differentiation, and apoptosis. The clinical significance of N1-acetylspermine is being increasingly recognized. Abnormal levels of this metabolite have been linked to cancer, neurodegenerative diseases, and other metabolic disorders. Its measurement in biological fluids such as urine and blood can provide valuable insight into disease states and therapeutic responses [42]. N1-acetylspermine has been found to play a significant role in cancer development by promoting tumor growth and metastasis through its influence on cell proliferation and apoptosis [43]. Additionally, it can modulate the host immune response, potentially impacting the tumor microenvironment. Elevated levels of N1-acetylspermine can suppress immune cell function, aiding in tumor immune evasion [44].

The balance between F-1,6-BP and F-2,6-BP is crucial for maintaining metabolic homeostasis. These metabolites facilitate ATP production and influence various cellular processes such as apoptosis, cell proliferation, and response to hypoxia. Dysregulation of their levels can lead to metabolic disorders, including diabetes and cancer [45]. F-1,6-BP and F-2,6-BP play critical roles in cancer metabolism by supporting the high glycolytic rates observed in tumor cells, known as the Warburg effect [46]. This enhanced glycolysis provides energy and biosynthetic precursors necessary for rapid cell proliferation. Furthermore, these metabolites can influence the host's immune response by altering the metabolism and function of immune cells [47].

Spermidine has been implicated in cancer development due to its role in cell proliferation and the inhibition of apoptosis. It can also modulate the host immune response, enhancing the antitumor activity of immune cells. Increased spermidine levels have been shown to support tumor growth, whereas reducing its levels can impair tumor progression. Furthermore, spermidine can influence autophagy, which can promote or inhibit cancer, depending on the context [48].

Histidine, acetylcholine, GTP, ATP, and UDP also enhance the host's immune response to tumor cells by producing reactive oxygen species (ROS) [49]. The mice that received xylitol via osmotic pumps exhibited higher levels of these metabolites, as mentioned earlier, in their tumors. Histidine, an amino acid, serves as a precursor for synthesizing histamine, which can activate immune cells and trigger ROS production, thereby contributing to the immune-mediated killing of cancer cells [50–52]. Acetylcholine, a neurotransmitter, has been shown to modulate immune cell activity and promote ROS generation, enhancing immune cells' cytotoxicity against tumor cells [53]. GTP and its derivatives, such as dGTP, are essential for activating G-proteins, which are involved in various signaling pathways, including those that regulate ROS production. Elevated levels of GTP and dGTP can enhance the immune response by promoting ROS-mediated tumor cell death [54–57]. ATP, a critical energy molecule, can also act as a signaling molecule that induces ROS production

in immune cells, thereby increasing their antitumor activity [58–60]. UDP, a nucleotide sugar, is involved in glycosylation processes that can modulate immune cell function and ROS production, enhancing the immune response to tumor cells [61].

Osmotic minipumps could, theoretically, be inserted into large tumors to deliver a constant supply of xylitol, which inhibits the growth of specific cancer cell lines without any side effects, if a beneficial effect on tumor growth is discovered. Alternatively, xylitol could be systemically administered during the treatment phase along with standard-of-care therapy, followed by using dietary xylitol supplements to prevent recurrence. Xylitol is absorbed in the small intestine through passive diffusion, which does not require energy. The efficiency of xylitol absorption is influenced by several factors, including other nutrients and the overall health of the intestinal mucosa [62]. This absorption mechanism is consistent with the behavior of other sugar alcohols, which are also absorbed through passive diffusion [63]. Xylitol has been shown to influence the gut microbiota composition in mice. Uebanso et al. reported that xylitol consumption changes the populations of beneficial and harmful bacteria in the gut [64]. These changes can influence digestive health and immune function, as gut microbiota plays a crucial role in these processes [65].

The digestion of xylitol primarily occurs in the liver, where it is converted into D-xylulose through the action of xylitol dehydrogenase. The half-life of xylitol in plasma is relatively short, typically ranging from 30 min to 1 h [66]. This rapid clearance is attributed to its efficient utilization in metabolic pathways and excretion through the kidneys. This metabolic pathway was detailed by Amo et al. (2011), who highlighted the role of xylitol dehydrogenase in facilitating the conversion process [67]. The conversion of xylitol into D-xylulose allows it to enter the pentose phosphate pathway, which is essential for cellular metabolism and the production of nucleotides [68]. In the liver, xylitol is phosphorylated and metabolized to xylulose 5-phosphate (Xu5P), an intermediate of the nonoxidative branch of the pentose phosphate pathway [69]. The xylitol metabolite Xu5P specifically activates both nuclear transport and the DNA-binding activities of carbohydrate response element binding protein. Studies have shown that xylitol can influence metabolic pathways, particularly those involved in energy production and immune regulation [66,67]. These changes can influence digestive health and immune function as the gut microbiota plays a crucial role in these processes. Delivering xylitol directly via ALZET mini osmotic pumps eliminated dietary variables and reduced potential confounders, especially those originating from the gut microbiome. The absorption and digestion of xylitol in mice involve complex processes influenced by various factors, including the presence of other nutrients, the health of the intestinal mucosa, and the animal's overall metabolic state [65]. However, xylitol may be a safe alternative to sucrose for patients who desire sweet-tasting foods. Additionally, the consumption of high-sucrose foods should be discouraged, and xylitol-containing products, as well as fruits and vegetables, should be encouraged among patients with cancer. Previous studies have demonstrated that xylitol inhibits the growth of certain cancers [24–26] and is readily incorporated into the diet, replacing sucrose and fructose. In the present study, the survival times of xylitol-treated mice were up to 35% higher than those of control mice, although the difference was not statistically significant. A larger sample size may yield statistically significant results in this type of biological study, which often involves numerous potential confounders.

This study, using a syngeneic mouse model to examine the effects of osmotic pump-delivered xylitol on malignant melanoma, faces several critical limitations. First, the inherent differences between murine and human physiology—particularly in immune response, tumor microenvironment, and metabolic pathways—limit the translational relevance of the findings. Second, the small sample size reduces statistical power, making it difficult to detect meaningful differences or confidently attribute observed effects to xylitol rather

than random variation. Without adequate replication and robust statistical significance, conclusions remain speculative. Additionally, animal studies often fail to account for the genetic and environmental heterogeneity seen in human populations, further constraining their applicability to clinical settings. These limitations underscore the need for cautious interpretation and follow-up studies in more representative models.

Extensive clinical trials should be considered to evaluate the benefits of xylitol, following confirmation by further research using cancer cell lines and syngeneic mouse models. No noticeable side effects of the xylitol treatment were found in the experimental group. The controls received 0.9% saline but the tonicity difference versus 10% w/v xylitol in saline would be inconsequential in systemic subcutaneous delivery and the very low daily mass (0.624 mg) make energy effects negligible (~0.0015 kcal/day).

5. Conclusions

We can hypothesize from the results of this preliminary study that xylitol has the potential to be an adjunct to oncological treatment and should be further investigated. An osmotic minipump (ALZET) provided systemic exposure to 10% w/v xylitol in saline solution, which temporarily reduced the growth of malignant melanoma tumors and may have increased the survivability of xylitol-treated mice; however, the results were not statistically significant. The sample size may have affected the statistical results as did the tumor size restriction for euthanasia at 2000 mm^3. Future large-scale studies with syngeneic models are warranted to evaluate the safety and efficacy of supplemental xylitol as an adjunct in cancer treatment.

Author Contributions: M.C.—conceptualization, original draft and funding, A.C.—draft review, E.D.—investigation and data analysis, N.G.—review of draft and data analysis. All authors have read and agreed to the published version of the manuscript.

Funding: Swanson Fund, a private, unrestricted fund at Northwestern University for Research. This work was supported by the Developmental Therapeutics Core at Northwestern University and the Robert H. Lurie Comprehensive Cancer Center support grant (NCI CA060553). Metabolomics services were performed by the Metabolomics Core Facility at Robert H. Lurie Comprehensive Cancer Center of Northwestern University.

Institutional Review Board Statement: I confirm that I have received ethical clearance for my abstract and declared conflicts of interest. The IACUC reviewed and approved this animal study. This research was conducted in strict accordance with ethical standards and guidelines for animal experimentation. All procedures performed in animal studies complied with the ethical standards of the institution where the studies were conducted. Efforts were made to minimize animal suffering and reduce the number of animals used. The Institutional Animal Care and Use Committee at Northwestern University approved all animal handling and experimental protocols.

Informed Consent Statement: Not applicable.

Data Availability Statement: Data are available at Metabolomics Core Facility (MCF) at Robert H. Lurie Comprehensive Cancer Center of Northwestern University. Contact Mark Cannon for details: drmarkcannon@outlook.com.

Acknowledgments: Funding—acknowledging Swanson Fund contributions by Lon Jones, Michael Milligan, and R. William Cornell. Thanks to Navdeep Chandel, Metabolic Core Facility, Northwestern University, for the kind suggestions and assistance.

Conflicts of Interest: The authors declare no conflicts of interest.

References

1. Milgrom, P.; Ly, K.A.; Rothen, M. Xylitol and its vehicles for public health needs. *Adv. Dent. Res.* **2009**, *21*, 44–47. [CrossRef]
2. Mooradian, A.D.; Smith, M.; Tokuda, M. The role of artificial and natural sweeteners in reducing the consumption of table sugar: A narrative review. *Clin. Nutr. eSPen* **2017**, *18*, 1–8. [CrossRef] [PubMed]
3. Knuuttila, M.L.E.; Makinen, K.K. Effect of xylitol on the growth and metabolism of *Streptococcus mutans*. *Caries Res.* **1975**, *9*, 177–189. [CrossRef]
4. Ly, K.A.; Milgrom, P.; Rothen, M. Xylitol, sweeteners, and dental caries. *Pediatr. Dent.* **2006**, *28*, 154–163.
5. Bradshaw, D.J.; Marsh, P.D. Effect of sugar alcohols on the composition and metabolism of a mixed culture of oral bacteria grown in a chemostat. *Caries Res.* **1994**, *28*, 251–256. [CrossRef]
6. Soderling, E.M. Xylitol, mutans streptococci, and dental plaque. *Adv. Dent. Res.* **2009**, *21*, 74–78. [CrossRef]
7. Scheinin, A. Caries control through the use of sugar substitutes. *Int. Dent. J.* **1976**, *26*, 4–13.
8. Makinen, K.K.; Isotupa, K.P.; Kivilompolo, T.; Makinen, P.L.; Toivanen, J.; Soderling, E. Comparison of erythritol and xylitol saliva stimulants in the control of dental plaque and mutans streptococci. *Caries Res.* **2001**, *35*, 129–135. [CrossRef]
9. Isokangas, P.; Alanen, P.; Tiekso, J.; Mäkinen, K.K. Xylitol chewing gum in caries prevention: A field study in children. *J. Am. Dent. Assoc.* **1988**, *11*, 315–320. [CrossRef]
10. Burt, B.A. The use of sorbitol- and xylitol-sweetened chewing gum in caries control. *J. Am. Dent. Assoc.* **2006**, *137*, 190–196. [CrossRef]
11. Makinen, K.K.; Isotupa, K.P.; Kivilompolo, T.; Makinen, P.L.; Murtomaa, S.; Petaja, J.; Toivanen, J.; Soderling, E. The effect of polyol-combinant saliva stimulants on *S. mutans* levels in plaque and saliva of patients with mental retardation. *Spec. Care Dent.* **2002**, *22*, 187–193. [CrossRef] [PubMed]
12. Makinen, K.K.; Saag, M.; Isotupa, K.P.; Olak, J.; Nommela, R.; Soderling, E.; Makinen, P.L. Similarity of the effects of erythritol and xylitol on some risk factors of dental caries. *Caries Res.* **2005**, *39*, 207–215. [CrossRef] [PubMed]
13. Janakiram, C.; Deepan Kumar, C.V.; Joseph, J. Xylitol in preventing dental caries: A systematic review and meta-analyses. *J. Nat. Sci. Biol. Med.* **2017**, *8*, 16–21. [CrossRef] [PubMed]
14. Kõljalg, S.; Smidt, I.; Chakrabarti, A.; Bosscher, D.; Mändar, R. Exploration of singular and synergistic effect of xylitol and erythritol on causative agents of dental caries. *Sci. Rep.* **2020**, *10*, 6297. [CrossRef]
15. Mäkinen, K.K. Sugar alcohols and prevention of oral diseases–comments and rectifications. *Oral Health Care* **2017**, *2*, 1–8. [CrossRef]
16. Salli, K.; Lehtinen, M.J.; Tiihonen, K.; Ouwehand, A.C. Xylitol's health benefits beyond dental health: A comprehensive review. *Nutrients* **2019**, *11*, 1813. [CrossRef]
17. Meng, C.; Bai, C.; Brown, T.D.; Hood, L.E.; Tian, Q. Human gut microbiota and gastrointestinal cancer. *Genom. Proteom. Bioinform.* **2018**, *16*, 33–49. [CrossRef]
18. Tsai, Y.L.; Lin, T.L.; Chang, C.J.; Wu, T.R.; Lai, W.F.; Lu, C.C.; Lai, H.C. Probiotics, prebiotics and amelioration of diseases. *J. Biomed. Sci.* **2019**, *26*, 3. [CrossRef]
19. Yadav, M.K.; Kumari, I.; Singh, B.; Sharma, K.K.; Tiwari, S.K. Probiotics, prebiotics and synbiotics: Safe options for next-generation therapeutics. *Appl. Microbiol. Biotechnol.* **2022**, *106*, 505–521. [CrossRef]
20. Liu, X.; Chen, Y.; Zhang, S.; Dong, L. Gut microbiota-mediated immunomodulation in tumor. *J. Exp. Clin. Cancer Res.* **2021**, *40*, 221. [CrossRef]
21. Abreu, M.T.; Peek, R.M., Jr. Gastrointestinal malignancy and the microbiome. *Gastroenterology* **2014**, *146*, 1534–1546.e3. [CrossRef] [PubMed]
22. Zhou, C.B.; Zhou, Y.L.; Fang, J.Y. Gut microbiota in cancer immune response and immunotherapy. *Trends Cancer* **2021**, *7*, 647–660. [CrossRef] [PubMed]
23. Ting, N.L.; Lau, H.C.; Yu, J. Cancer pharmacomicrobiomics: Targeting microbiota to optimise cancer therapy outcomes. *Gut.* **2022**, *71*, 1412–1425. [CrossRef] [PubMed]
24. Park, E.; Park, M.H.; Na, H.S.; Chung, J. Xylitol induces cell death in lung cancer A549 cells by autophagy. *Biotechnol. Lett.* **2015**, *37*, 983–990. [CrossRef]
25. Tomonobu, N.; Komalasari, N.L.G.Y.; Sumardika, I.W.; Jiang, F.; Chen, Y.; Yamamoto, K.I.; Kinoshita, R.; Murata, H.; Inoue, Y.; Sakaguchi, M. Xylitol acts as an anticancer monosaccharide to induce selective cancer death via regulation of the glutathione level. *Chem. Biol. Interact.* **2020**, *324*, 109085. [CrossRef]
26. Sahasakul, Y.; Angkhasirisap, W.; Lam-Ubol, A.; Aursalung, A.; Sano, D.; Takada, K.; Trachootham, D. Partial substitution of glucose with xylitol prolongs survival and suppresses cell proliferation and glycolysis of mice bearing orthotopic xenograft of oral cancer. *Nutrients* **2022**, *14*, 2023. [CrossRef]

27. Mehnert, H.; Förster, H.; Dehmel, K.H. The effect of intravenous administration of xylitol solutions in normal persons and in patients with liver diseases and diabetes mellitus. In Proceedings of the International Symposium on Metabolism, Physiology, and Clinical Use of Pentoses and Pentitols, Hakone, Japan, 27–29 August 1967; Horecker, B.L., Lang, K., Takagi, Y., Eds.; Springer: Berlin/Heidelberg, Germany, 1969; pp. 293–302.
28. Sato, J.; Wang, Y.M.; van Eys, J. Metabolism of xylitol and glucose in rats bearing hepatocellular. *Cancer Res.* **1981**, *41*, 3192–3199.
29. Yi, E.Y.; Kim, Y.J. Xylitol inhibits in vitro and in vivo angiogenesis by suppressing the NF-κB and Akt signaling pathways. *Int. J. Oncol.* **2013**, *43*, 315–320. [CrossRef]
30. Ylikahri, R.H.; Leino, T. Metabolic interactions of xylitol and ethanol in healthy males. *Metabolism* **1979**, *28*, 25–29. [CrossRef]
31. Hutcheson, R.M.; Reynolds, V.H.; Touster, O. The reduction of L-xylulose to xylitol by guinea pig liver mitochondria. *J. Biol. Chem.* **1956**, *221*, 697–709. [CrossRef]
32. Ahuja, V.; Macho, M.; Ewe, D.; Singh, M.; Saha, S.; Saurav, K. Biological and pharmacological potential of xylitol: A molecular insight of unique metabolism. *Foods* **2020**, *9*, 1592. [CrossRef] [PubMed]
33. Makinen, K.K.; Soderling, E. A quantitative study of mannitol, sorbitol, xylitol, and xylose in wild berries and commercial fruits. *J. Food Sci.* **1980**, *45*, 367–374. [CrossRef]
34. Islam, M.S. Effects of xylitol as a sugar substitute on diabetes-related parameters in nondiabetic rats. *J. Med. Food* **2011**, *14*, 505–511. [CrossRef] [PubMed]
35. Park, E.; Na, H.S.; Kim, S.M.; Wallet, S.; Cha, S.; Chung, J. Xylitol, an anticaries agent, exhibits potent inhibition of inflammatory responses in human THP-1-derived macrophages infected with *Porphyromonas gingivalis*. *J. Periodontol.* **2014**, *85*, e212–e223. [CrossRef]
36. Trachootham, D.; Chingsuwanrote, P.; Yoosadiang, P.; Mekkriangkrai, D.; Ratchawong, T.; Buraphacheep, N.; Kijanukul, S.; Saekhow, S.; Pongpitchayadej, O.; Vongvachvasin, K.; et al. Partial substitution of glucose with xylitol suppressed the glycolysis and selectively inhibited the proliferation of oral cancer cells. *Nutr. Cancer* **2017**, *69*, 862–872. [CrossRef]
37. Qusa, M.H.; Siddique, A.B.; Nazzal, S.; El Sayed, K.A. Novel olive oil phenolic (−)-oleocanthal(+)-xylitol-based solid dispersion formulations with potent oral anti-breast cancer activities. *Int. J. Pharm.* **2019**, *569*, 118596. [CrossRef]
38. Ireson, C.R.; Alavijeh, M.S.; Palmer, A.M.; Fowler, E.R.; Jones, H.J. The role of mouse tumour models in the discovery and development of anticancer drugs. *Br. J. Cancer* **2019**, *121*, 101–108. [CrossRef]
39. Cogels, M.M.; Rouas, R.; Ghanem, G.E.; Martinive, P.; Awada, A.; van Gestel, D.; Krayem, M. Humanized mice as a valuable pre-clinical model for cancer immunotherapy research. *Front. Oncol.* **2021**, *11*, 784947. [CrossRef]
40. Wang, Y.; Qi, H.; Liu, Y.; Duan, C.; Liu, X.; Xia, T.; Chen, D.; Piao, H.L.; Liu, H.X. The double-edged roles of ROS in cancer prevention and therapy. *Theranostics* **2021**, *11*, 4839–4857. [CrossRef]
41. AHegde, S.S.; Chandler, J.; Vetting, M.W.; Yu, M.; Blanchard, J.S. Mechanistic and structural analysis of human spermidine/spermine N1-acetyltransferase. *Biochemistry* **2007**, *46*, 7187–7195. [CrossRef]
42. Ni, Y.Q.; Liu, Y.S. New Insights into the Roles and Mechanisms of Spermidine in Aging and Age-Related Diseases. *Aging Dis.* **2021**, *12*, 1948–1963. [CrossRef] [PubMed]
43. Holbert, C.E.; Cullen, M.T.; Casero, R.A., Jr.; Stewart, T.M. Polyamines in cancer: Integrating organismal metabolism and antitumour immunity. Nature reviews. *Cancer* **2022**, *22*, 467–480. [CrossRef] [PubMed]
44. Lian, J.; Liang, Y.; Zhang, H.; Lan, M.; Ye, Z.; Lin, B.; Qiu, X.; Zeng, J. The role of polyamine metabolism in remodeling immune responses and blocking therapy within the tumor immune microenvironment. *Front. Immunol.* **2022**, *13*, 912279. [CrossRef] [PubMed]
45. Timson, D.J. Fructose 1,6-bisphosphatase: Getting the message across. *Biosci. Rep.* **2019**, *39*, BSR20190124. [CrossRef]
46. Cho, E.S.; Cha, Y.H.; Kim, H.S.; Kim, N.H.; Yook, J.I. The Pentose Phosphate Pathway as a Potential Target for Cancer Therapy. *Biomol. Ther.* **2018**, *26*, 29–38. [CrossRef]
47. Bartrons, R.; Simon-Molas, H.; Rodríguez-García, A.; Castaño, E.; Navarro-Sabaté, À.; Manzano, A.; Martinez-Outschoorn, U.E. Fructose 2,6-Bisphosphate in Cancer Cell Metabolism. *Front. Oncol.* **2018**, *8*, 331. [CrossRef]
48. Prasher, P.; Sharma, M.; Singh, S.K.; Gulati, M.; Chellappan, D.K.; Rajput, R.; Gupta, G.; Ydyrys, A.; Kulbayeva, M.; Abdull Razis, A.F.; et al. Spermidine as a promising anticancer agent: Recent advances and newer insights on its molecular mechanisms. *Front. Chem.* **2023**, *11*, 1164477. [CrossRef]
49. Schmidt, D.R.; Patel, R.; Kirsch, D.G.; Lewis, C.A.; Vander Heiden, M.G.; Locasale, J.W. Metabolomics in cancer research and emerging applications in clinical oncology. *CA Cancer J. Clin.* **2021**, *71*, 333–358. [CrossRef]
50. Oldenburg, O.; Qin, Q.; Sharma, A.R.; Cohen, M.V.; Downey, J.M.; Benoit, J.N. Acetylcholine leads to free radical production dependent on K(ATP) channels, G(i) proteins, phosphatidylinositol 3-kinase and tyrosine kinase. *Cardiovasc. Res.* **2002**, *55*, 544–552. [CrossRef]
51. Liu, P.; Huang, F.; Lin, P.; Liu, J.; Zhou, P.; Wang, J.; Sun, H.; Xing, F.; Ma, H. Histidine metabolism drives liver cancer progression via immune microenvironment modulation through metabolic reprogramming. *J. Transl. Med.* **2025**, *23*, 262. [CrossRef]

52. Zanoni, M.; Pegoraro, A.; Adinolfi, E.; De Marchi, E. Emerging roles of purinergic signaling in anti-cancer therapy resistance. *Front. Cell Dev. Biol.* **2022**, *10*, 1006384. [CrossRef]
53. Cox, M.A.; Bassi, C.; Saunders, M.E.; Nechanitzky, R.; Morgado-Palacin, I.; Zheng, C.; Mak, T.W. Beyond neurotransmission: Acetylcholine in immunity and inflammation. *J. Intern. Med.* **2020**, *287*, 120–133. [CrossRef] [PubMed]
54. Purves, D.; Augustine, G.J.; Fitzpatrick, D.; Katz, L.; LaMantia, A.; McNamara, J.; Williams, S. (Eds.) G-Proteins and Their Molecular Targets. In *Neuroscience*, 2nd ed.; Sinauer Associates: Sunderland, MA, USA, 2001. Available online: https://www.ncbi.nlm.nih.gov/books/NBK10832/ (accessed on 5 May 2025).
55. Snezhkina, A.V.; Kudryavtseva, A.V.; Kardymon, O.L.; Savvateeva, M.V.; Melnikova, N.V.; Krasnov, G.S.; Dmitriev, A.A. ROS Generation and Antioxidant Defense Systems in Normal and Malignant Cells. *Oxidative Med. Cell. Longev.* **2019**, *2019*, 6175804. [CrossRef] [PubMed]
56. Yagüe-Capilla, M.; Rudd, S.G. Understanding the interplay between dNTP metabolism and genome stability in cancer. *Dis. Models Mech.* **2024**, *17*, dmm050775. [CrossRef] [PubMed]
57. He, H.; Huang, J.; Wu, S.; Jiang, S.; Liang, L.; Liu, Y.; Liu, W.; Xie, L.; Tao, Y.; Jiang, Y.; et al. The roles of GTPase-activating proteins in regulated cell death and tumor immunity. *J. Hematol. Oncol.* **2021**, *14*, 171. [CrossRef]
58. Novak, I. ATP as a signaling molecule: The exocrine focus. *Physiology* **2003**, *18*, 12–17. [CrossRef]
59. Yegutkin, G.G.; Boison, D. ATP and Adenosine Metabolism in Cancer: Exploitation for Therapeutic Gain. *Pharmacol. Rev.* **2022**, *74*, 797–822. [CrossRef]
60. Savio, L.E.B.; Leite-Aguiar, R.; Alves, V.S.; Coutinho-Silva, R.; Wyse, A.T.S. Purinergic signaling in the modulation of redox biology. *Redox Biol.* **2021**, *47*, 102137. [CrossRef]
61. Scolaro, T.; Manco, M.; Pecqueux, M.; Amorim, R.; Trotta, R.; Van Acker, H.H.; Van Haele, M.; Shirgaonkar, N.; Naulaerts, S.; Daniluk, J.; et al. Nucleotide metabolism in cancer cells fuels a UDP-driven macrophage cross-talk, promoting immunosuppression and immunotherapy resistance. *Nat. Cancer* **2024**, *5*, 1206–1226. [CrossRef]
62. Bordier, V.; Teysseire, F.; Senner, F.; Schlotterbeck, G.; Drewe, J.; Beglinger, C.; Wölnerhanssen, B.K.; Meyer-Gerspach, A.C. Absorption and Metabolism of the Natural Sweeteners Erythritol and Xylitol in Humans: A Dose-Ranging Study. *Int. J. Mol. Sci.* **2022**, *23*, 9867. [CrossRef]
63. Wölnerhanssen, B.K.; Meyer-Gerspach, A.C.; Beglinger, C.; Islam, M.S. Metabolic effects of the natural sweeteners xylitol and erythritol: A comprehensive review. *Crit. Rev. Food Sci. Nutr.* **2020**, *60*, 1986–1998. [CrossRef]
64. Uebanso, T.; Kano, S.; Yoshimoto, A.; Naito, C.; Shimohata, T.; Mawatari, K.; Takahashi, A. Effects of Consuming Xylitol on Gut Microbiota and Lipid Metabolism in Mice. *Nutrients* **2017**, *9*, 756. [CrossRef]
65. Ma, P.; Sun, W.; Sun, C.; Tan, J.; Dong, X.; He, J.; Ali, A.; Chen, M.; Zhang, L.; Wu, L.; et al. Using gut microbiota and non-targeted metabolomics techniques to study the effect of xylitol on alleviating DSS-induced inflammatory bowel disease in mice. *BMC Immunol.* **2025**, *26*, 18. [CrossRef]
66. Amo, K.; Arai, H.; Uebanso, T.; Fukaya, M.; Koganei, M.; Sasaki, H.; Yamamoto, H.; Taketani, Y.; Takeda, E. Effects of xylitol on metabolic parameters and visceral fat accumulation. *J. Clin. Biochem. Nutr.* **2011**, *49*, 1–7. [CrossRef] [PubMed]
67. Ylikahri, R. Metabolic and nutritional aspects of xylitol. *Adv. Food Res.* **1979**, *25*, 159–180. [CrossRef]
68. Kabashima, T.; Kawaguchi, T.; Wadzinski, B.E.; Uyeda, K. Xylulose 5-phosphate mediates glucose-induced lipogenesis by xylulose 5-phosphate-activated protein phosphatase in rat liver. *Proc. Natl. Acad. Sci. USA* **2003**, *100*, 5107–5112. [CrossRef] [PubMed]
69. Jakob, A.; Williamson, J.R.; Asakura, T. Xylitol metabolism in perfused rat liver. *J. Biol. Chem.* **1971**, *246*, 7623–7631. [CrossRef] [PubMed]

Disclaimer/Publisher's Note: The statements, opinions and data contained in all publications are solely those of the individual author(s) and contributor(s) and not of MDPI and/or the editor(s). MDPI and/or the editor(s) disclaim responsibility for any injury to people or property resulting from any ideas, methods, instructions or products referred to in the content.